PERIÓDICO TCHÊ QUÍMICA
ARTIGO ORIGINAL

ANÁLISE GEOMÉTRICA DO FLUXO SUPERSÔNICO EM DOIS CORPOS AXIALMENTE SIMÉTRICOS USANDO O MÉTODO DE PROCESSAMENTO DE IMAGEM DIGITAL

GEOMETRY ANALYSIS OF SUPERSONIC FLOW AROUND TWO AXIALLY SYMMETRICAL BODIES USING THE DIGITAL IMAGE PROCESSING METHOD

ГЕОМЕТРИЧЕСКИЙ АНАЛИЗ СВЕРХЗВУКОВОГО ОБТЕКАНИЯ ДВУХ ТЕЛ ВРАЩЕНИЯ С ПРИВЛЕЧЕНИЕМ МЕТОДА ЦИФРОВОЙ ОБРАБОТКИ ИЗОБРАЖЕНИЯ

BODRYSHEV, Valeriy V.[1*]; KORZHOV, Nikolay P.[2]; NARTOVA, Lidiya G.[3]; RABINSKIY, Lev N.[4];

[1,2,3,4] Moscow Aviation Institute (National Research University), Department of Engineering Graphics, Moscow – Russian Federation

** Correspondence author*
e-mail: NioBVV@mail.ru

Received 03 September 2019; received in revised form 27 October 2019; accepted 28 October 2019

RESUMO

O artigo é dedicado ao estudo das leis geométricas de interseção de duas ondas de choque oblíquas formadas durante o fluxo supersônico em torno de dois corpos localizados no ângulo de ataque zero. Foram determinadas as coordenadas dos pontos de contato das ondas de choque com as superfícies dos modelos dos corpos axissimétricos. Os sistemas de análise de decisão e suporte à decisão são baseados na atração dos resultados do processamento de fotos (quadros de vídeo) pelo parâmetro da intensidade da imagem. Esse método permite determinar os ângulos de inclinação das ondas de choque com um alto grau de probabilidade e, portanto, identificar com mais precisão os pontos de contato da onda de choque com a superfície investigada. Foi feita uma análise dos quadros de vídeo da interação das ondas de choque usando o método de processamento de imagem digital de acordo com o parâmetro de intensidade da imagem. Foram apresentadas fórmulas que determinam o ponto de interseção das ondas de choque decorrentes do movimento supersônico de dois corpos axissimétricos próximos um do outro. As coordenadas do ponto de contato da onda de choque de saída com a superfície do segundo objeto foram determinadas levando em consideração a diferença nos ângulos de inclinação das ondas de choque de entrada e de saída. A disponibilidade de estatísticas suficientes permitiu identificar relações teóricas entre a vazão do gás, os parâmetros geométricos dos objetos, as distâncias entre eles, densidade, pressão e intensidade da imagem nas fotografias. O método de processamento de imagem digital pode ser aplicado à análise de ondas de choque durante o fluxo supersônico em torno de corpos com uma extremidade "embotada". A frente da onda de choque, neste caso, é descrita por uma curva de segunda ordem, na análise da qual é necessário selecionar uma parte dessa curva, substituindo-a com certa precisão por um segmento de linha reta (linha Mach).

Palavras-chave: *densidade de fluxo de gás, intensidade de imagem, processamento digital de imagens de sombra, onda de choque, interferência aerodinâmica.*

ABSTRACT

The scientific paper covers the research of the geometric laws of the intersection of two angle shock waves formed upon supersonic flow with zero incidence of two bodies. The positions of shock waves engaging with the surfaces of the models of axially symmetrical bodies are determined. Systems of analysis and decision support are based on the involvement of photographs (video frames) processing results by the image intensity parameter. This method facilitates the identification of the shock wave angle with a higher rate of probability, and, therefore, the more precise definition of the engagement points of the shock wave with the researched surface. This paper analyses the video frames of the interaction of shock waves using the digital image processing method by the image intensity parameter, the formulas determining the intersection point of shock waves, that occur upon the supersonic motion of two axially symmetric bodies near each other, are determined. The positions of the point of contact of the outgoing shock wave with the surface of the second object were determined, factoring in the difference in the the incoming and outgoing shock wave angles. The availability of sufficient statistics allowed to identify theoretical relationships between the gas flow rate, the geometric

DOI: 10.52571/PTQ.v16.n33.2019.556_Periodico33_pgs_541_548.pdf

parameters of objects, the distances between them, density, pressure and image intensity in photographs. The method of digital image processing can be applied to the analysis of shock waves during the flow around a supersonic stream of bodies with a "blunt" end. The shock wave front in this case is described by a second-order curve, upon the analysis of which it is necessary to select a portion of this curve, replacing it with some accuracy by a straight line segment (Mach line).

Keywords: *gas flow density, image intensity, digital processing of shadow images, compressive shock wave, aerodynamic interference.*

АННОТАЦИЯ

Статья посвящена исследованию геометрических законов пересечения двух косых скачков уплотнения, образующихся при сверхзвуковом обтекания расположенных при нулевом угле атаки двух тел. Определены координаты точек контакта ударных волн с поверхностями моделей осесимметричных тел. Системы анализа и поддержки принятия решений основываются на привлечении результатов обработки фотографий (видеокадров) по параметру интенсивность изображения. Данный метод позволяет определить углы наклона ударных волн с большой долей вероятности, и, следовательно, более точно выявить точки контакта ударной волны с исследуемой поверхностью. В работе был проведен анализ видеокадров взаимодействия ударных волн с применением метода цифровой обработки изображения по параметру интенсивность изображения, представлены формулы, определяющие точку пересечения ударных волн, возникающих при сверхзвуковом движении двух осесимметричных тел вблизи друг друга. Были определены координаты точки касания исходящего скачка уплотнения с поверхностью второго объекта с учетом отличия углов наклона приходящей и исходящей ударной волны. Наличие достаточной статистики позволило выявить теоретические зависимости между скоростью газового потока, геометрическими параметрами объектов, расстояниями между ними, плотностью, давлением и интенсивностью изображения на фотографиях. Метод цифровой обработки изображений может быть применен для анализа скачков уплотнения при обтекании сверхзвуковым потоком тел с «затупленным» концом. Фронт ударной волны в этом случае описывается кривой второго порядка, при анализе которой необходимо выделить участок этой кривой, заменив с некоторой точностью ее отрезком прямой линии (линией Маха).

Ключевые слова: *плотность газового потока, интенсивность изображения, цифровая обработка теневых снимков, скачок уплотнения, аэродинамическая интерференция.*

1. INTRODUCTION

The studies of supersonic flows implemented in conditions of a group flight of airborne vehicles under various conditions of their relative position refer to the problems of aerogas dynamics. A detailed analysis of the gas-dynamic structure of their interaction is important for explaining the effects of aerodynamic interference and predicting the forces and torques that arise (Dmitriev *et al.*, 2011; Babaytsev *et al.*, 2015). An in-depth study of the features of the development of such complex flows requires the involvement of both experimental and computational methods (Sokolov and Ryabinov, 2015).

In (Derunov *et al.,* 2009), the results of numerical calculations of supersonic flow around two axially symmetrical bodies located at angles of attack were compared with experimental data. The calculations were based on solving the Euler equations. In (Zabrodin *et al.,* 1995; Volkov and Derunov, 2005; Volkov and Derunov, 2006), the flow around two similar bodies at zero angle of attack was studied; in (Eremin *et al.,* 2002), the possibilities of numerical calculation of aerodynamics during the separation of rocket stages were shown. In (Volkov, 1998; Brodetsky *et al.,* 1998), the effects of aerodynamic interference with the surface of an axially symmetrical body with a conical head were studied, and in (Brodetsky *et al.,* 1999), two similar bodies. In (Chaplin *et al.,* 2016; Chaplin *et al.,* 2011; Chaplin, 2009; Bulat and Uskov, 2015), the results of a study of the models of axially symmetrical bodies with various configurations of the nose part streamlined by an air supersonic flow are presented.

The work includes both experimental results of blowing in a wind tunnel at M = 2.43, and calculations for various conditions of interaction between bodies. The forces and torques forcing on the model were measured for different variants of the arrangement of bodies, and dimensionless aerodynamic coefficients were calculated.

In this scientific paper, in order to study the processes of interaction of gas-dynamic shock waves of supersonic flow, using the method of digital processing of video frames is proposed (Tarasenko *et al.,* 2015; Bodryshev *et al.,* 2016; Tarasenko *et al.,* 2017; Bodryshev *et al.,* 2018). This method makes it possible to more accurately determine the angle of the shock wave on the Mach line (Bodryshev *et al.,* 2016; Bodryshev *et al.,* 2018; Rabinskiy and Tushavina, 2019b; Rabinskiy and Tushavina, 2019a; Nikitin *et al.,* 2019; Rabinskiy *et al.,* 2019), evaluate the “strength” of the crossing waves, their dependence on the geometry of the objects, and determine changes in the angles of shock waves after the point of impact. This allows us to more accurately calculate the coordinates of the engagement point of the shock wave peak with the surface of the "neighboring" object.

2. MATERIALS AND METHODS

2.1. Method for Determining the Geometric Parameters of the Compressive Shock Wave Zone

During the movement of supersonic axially symmetrical vehicles in conditions of a group flight, compressive shock waves arise in front of them, the shape of which depends on the fore part of a particular vehicle, the angle of the interaction of objects (Chaplin *et al.,* 2016). In front of the vehicle, which has an ogive shape, intermediate between a cone and an ellipsoid, which further turns into a cylindrical one, an attached conical compressive shock wave with a peak at the apex of the ogive-shaped body arises.

When flowing around bodies with a “blunt” end, the front of the shock wave is described by a quadric curve, in the analysis of which a section of this curve is usually distinguished, replacing with a certain accuracy by a straight line segment (the Mach line). When two or more similar vehicles move close to each other, interaction (interference) of compressive shock waves occurs, as a result of which shock waves have an effect on the bodies of moving vehicles. This leads to a change in the pressure field structure on the vehicle bodies, a change in the aerodynamic torque curves and, in the final version, it can lead to a change in their subsequent trajectories of motion, and increase the likelihood of a collision.

Figure 1 shows a diagram of a shock wave structure (*SWS*) formed in the space between models. The incoming shocks until they intersect preserve the shape of a classical cone. The generators of the cones until they intersect with each other constitute straight lines. The intersection line of the cones (shock waves) is a quartic curve. Beyond the intersection line, the shocks become quartic surfaces, shear surfaces, or the so-called extruded surfaces, i.e., surfaces formed by the displacement of an arbitrary generator along an arbitrary guide track. In this case, the generators of the shear surface are generators of a variable type (Figure 1, *b*).

2.2. Digital Image Processing Method for Assessing the Position of Crossing Shock Waves

Figure 2 shows the results of an experimental study on supersonic flow around two bodies (Chaplin *et al.,* 2016). Both bodies have the same shape in the fore part; the distance between the axes of the models is 2.94*D* (*D* is the diameter of the cylindrical part of the model). The displacement of the fore parts of the models relative to each other is $\Delta x = 0$. The angle between the axes of the models is $\psi = 0$.

For this option, the attached conical compressive shock waves with a peak at the apex of the ogive-shaped body should be identical to each other. The initial analysis of this photograph by the image intensity parameter showed the need to make adjustments to the initial experimental data given by the authors. Thus, the distance between the axes of the models in the area of the head parts is equal to 2.78*D*, the distance in the area of the tail parts is equal to 2.93*D*. That is, there is some deviation of the object axes from parallel alignment. It is also confirmed by the results of measuring the angles between incoming compressive shock waves.

3. RESULTS AND DISCUSSION:

3.1. The Geometric Parameters of the Compressive Shock Wave Zone

Let us consider the pattern of the intersection of oblique conical compressive shock waves formed by the movement of two identical objects with conical heads in the plane of symmetry (Figure 3). The rate of the first object M_1, the second object M_2. The distance between the model axes is equal to H. The displacement of the fore parts of the models relative to each other is Δx. The angle between the model axes is $\psi = 0$.

The angles between the generators of the attached conical compressive shock waves and their axes are called Mach angles. They are related to the Mach number according to the following ratios (Equations 1, 2). The coordinates of the point of intersection of two shock waves $A_0(x_0, y_0)$ are determined by solving two equations (Equation 3). When equating the right parts, Equation 4 is gotten.

The coefficients *c* and *d* are determined based on the values of the point coordinates $A_1(x_1, y_1)$ and $A_2(x_2, y_2)$ (Equations 5, 6). When solving Equations 1-5 consistently, the generalized equations for determining the coordinates x_0, y_0 (Equations 7, 8) are obtained. In this case, the distances H_1 and H_2 from the point of intersection of the shock waves $A_0(x_0, y_0)$ are determined by the dependencies (Equation 9).

When the values of the point coordinate $A_0(x_0, y_0)$ and the values of the angles θ and φ are known, the coordinates of the intersection points $A_3(x_3, y_3)$ and $A_4(x_4, y_4)$ of the outgoing shock waves with objects shall be defined according to dependencies (Equations 10, 11). The geometric calculations presented above proceed from the variant of the head parts of objects made in the form of a classical cone for which ratios (Equation 1) are valid. At the same time, in real constructions, the shape of the head part can differ significantly from the conical one and have, for example, the shape of an ogive-shaped body.

Therefore, when determining the values of the angles of the conical compressive shock waves outgoing from the nose parts of the objects, their correction is necessary. It is also necessary to know the exact values of the oblique angles θ and φ. A quantitative assessment of the angles of the compressive shock waves depending on the rate of the incoming flow can be performed using the method of digital processing of shadow images by the image intensity parameter. Such a method is given in (Tarasenko *et al.,* 2015). Further development and capability enhancement of its application for various problems of supersonic gas dynamics are presented in (Bodryshev *et al.,* 2016; Tarasenko *et al.,* 2017; Bodryshev *et al.,* 2018; Abashev *et al.,* 2018).

3.2. Assessing the Position of Crossing Shock Waves

Figure 2, *b* shows a photograph display of Figure 2, *a* in functional form $L = f(x, y)$. Here L is the image intensity. Further processing is performed as follows. The image area is divided into discrete cells. Each cell can contain from *1* to *n* pixels along the *x* axis and *1* to *m* pixels along the *y* axis. The cell size (*m* and *n*) depends on the necessary accuracy in estimating the value of the flow rate, and it is determined by practical rationality. Cell parameters *x*, *y* are fixed by the coordinates of its center or any angle of the cell (for example, the bottom-left angle). Thus, the image is stored in the form of a two-dimensional array (i.e., a matrix in size $m \times n$), in which each element with coordinates (*x*, *y*) corresponds to the accepted cell coordinate.

Since *L* for a shadow image characterizes the rate of change in the gas flow density (Tarasenko *et al.,* 2015; Bodryshev *et al.,* 2016), then the change in *L* determines the dynamics of the flow rate. Figure 4, *a*, as an example, shows graphs of the changes in *L* in longitudinal sections *1* and *2*. Section *2* passes through the point of intersection of the shock waves. In both sections, the graphs of the changes in the image intensity look identical when the flow passes through the compressive shock waves. The minimal intensities L_{1min}, L_{2min} are observed on the shock line (the flow rate is minimal, the pressure is maximal), immediately after the shock occurs the image intensities L_{1max} and L_{2max} are maximal (the flow rate increased, and the pressure decreased). But the length of the burst area of the image intensity is greater in section 2 ($\Delta 2$ is larger than $\Delta 1$ by about 2.5 times).

The amplitudes of increase and attenuation of the image intensity on the line of the compressive shock waves are larger when the flow passes the interference point of shock waves. Thus, the intensity of the *shock wave process*, which is characterized by the ratio of static pressures before and after the *shock wave process*, is higher when the flow passes the interference point. Most likely, this is the reason for the change in the values of the oblique angles of compressive shock waves after their interaction. Figure 4, *b* shows that after the shock wave interaction at point A, each of them continues to grow in the same direction as previously. The hypothesis that after shock waves encounter, each can be represented as one reflected from an imaginary plane passing through the intersection point of these shocks is not correct.

In order to determine the true oblique angle of the shock wave of the Mach cone, outgoing from the head of the object, it is necessary to obtain the exact direction of the straight line, which forms the Mach cone. For this purpose, the method of least squares by discrete points is used. It is expedient to apply two options for using this method based on the condition

(Figure 5) (Bodryshev *et al.,* 2016). Here L_i - the intensity in the *i*-th cell, L_{LV} - the limiting value of the intensity.

1. By the coordinates of the extreme cells in the initial stage of the shock wave.

2. By the coordinates of the cells that determine the beginning of the shock wave using the Freeman chain code.

Here, the cells are defined as a sequence according to an eight-linked lattice. The equations of the line when using the method of least squares are as follows in Equations 12, 13. Hence the oblique angle of the compressive shock wave φ is in Equation 14 where N is the number of cells with measurement L_i. Thus, processing the "lines" 1-1, 1-2, 2-1, 2-2 (Figure 2) the angles $\alpha, \beta, \varphi, \theta$ are determined.

Using this method, all the angles of the lines of compressive shock waves before they intersect at point A_0 and after it were calculated. The obtained values of the angles of incoming and outgoing compressive shock waves are shown in Figure 2, *a*. The values of incoming compressive shock waves from identical test models are not equal to each other, and they differ from the value of the Mach cone angle, determined by the ratio (Equation 2).

At the claimed flow rate in the experiment under study, M = 2.43, the angles for both shocks should be 24.3°. The difference between the theoretical angle φ and the experimentally measured angle may be due to the fact that the shape of the head of the models under test has an ogive shape, rather than a conical shape, for which the angle of the Mach cone is determined. In addition, as shown above, the axes of the models during the test are not completely parallel. The digital image processing method can also be used to analyze compressive shock waves during a supersonic flow around bodies with a "blunt" end. The shock wave front, in this case, is described by a quadric curve, in the analysis of which it is necessary to separate a section of this curve, replacing it with a certain accuracy by a straight line segment (the Mach line).

4. CONCLUSIONS:

The analysis of video frames of the shock waves interaction was made using the method of digital image processing by the parameter image intensity. There are formulas that determine the point of intersection of shock waves arising from the supersonic motion of two axially symmetrical bodies close to each other. The angles of shock waves were determined both by the traditional method depending on the gas flow rate and by using the digital image processing method, which allows more accurate determination of the wave oblique angle before and after the point of intersection of the shock waves.

The coordinates of the point of contact of the outgoing compressive shock wave with the surface of the second object are determined, taking into account the difference in the oblique angles of the incoming and outgoing shock wave. This makes it possible to more accurately predict the distribution of pressure on the vehicle bodies and to calculate the aerodynamic torque characteristics.

The availability of sufficient statistics makes it possible to identify theoretical ratios between the gas flow rate, the geometric parameters of objects, the distances between them, density, pressure, and image intensity in photographs.

5. ACKNOWLEDGMENTS:

This work has been partially supported by RFBR, project No. 17-01-00837.

6. REFERENCES:

1. Babaytsev, A.V., Kornev, Y.V., Semenov, N.A. *International Journal of Nanomechanics Science and Technology,* **2015**, *6*(4), 261-280.
2. Bodryshev, V.V., Abashev, V.M., Korzhov, N.P., Tarasenko, O.S. *Bulletin of Tula State University. Section Engineering,* **2018**, *6*, 458–467.
3. Bodryshev, V.V., Abashev, V.M., Tarasenko, O.S., Mirolyubova, T.I. *Electronic Journal “Transactions of Moscow Aviation Institute”,* **2016**, *88*, http://trudymai.ru/published.php?ID=70428, accessed 20 April 2019.
4. Brodetsky, M.D., Derunov, E.K., Kharitonov, A.M., Zabrodin, A.V., Lutsky, A.E. *Thermophysics and Aeromechanics*, **1998**, *5(3),* 301–306.
5. Brodetsky, M.D., Derunov, E.K., Kharitonov, A.M., Zabrodin, A.V., Lutsky, A.E. *Thermophysics and Aeromechanics*, **1999**, *6(2),* 165–172.
6. Bulat, P.V., Uskov, V.N. *Collection of scientific articles of the International*

Scientific Division of the ITMO University "Mechanics and Energy Systems", **2015**, 24–39.

7. Chaplin, R., *Aerodynamic Interference Between High-Speed SlenderBodies*, Ph.D. Thesis, Cranfield University, Cranfield, England, **2009**.
8. Chaplin, R., MacManus, D., Leopold, F., Martinez, B., Gauthier, T., Birch, T. *Computers and Fluids,* **2011**, *50(1)*, 155–174.
9. Chaplin, R., MacManus, D.G., Leopold, F., Martinez, B., Gauthier, T., Birch, T. *AIAA Journal*, **2016**, *54(7),* 2017–2033.
10. Derunov, E.K., Volkov, V.F., Zheltovodov, A.A., Maximov, A.I.. *Thermophysics and Aeromechanics,* **2009**, *16(1),* 13–20
11. Dmitriev, A.I., Skvortsov, AA., Koplak, O.V., Morgunov, R.B., Proskuryakov, I.I. *Physics of the Solid State*, **2011**, *53*(8), 1547-1553.
12. Eremin, V.V., Mikhalin, V.A., Rodionov, A.V. *Aeromechanics and Gas Dynamics*, **2002**, *1*, 24–35.
13. Nikitin, P.V., Tushavina, O.V., Shkuratenko, A.A. *INCAS Bulletin*, **2019**, *11,* 191–201, DOI: 10.13111/2066-8201.2019.11.S.19.
14. Rabinskiy, L. N., Tushavina, O. V. *INCAS Bulletin,* **2019a**, 11, 203–211, DOI: 10.13111/2066-8201.2019.11.S.20;
15. Rabinskiy, L.N., Tushavina, O.V., Fedotenkov, G.V. *Asia Life Sciences*, **2019**, *19(1),* 149–162.
16. Rabinskiy, L.N., Tushavina, O.V. *STİN*, **2019b**, *4*, 22–26.
17. Sokolov, N.S., Ryabinov, V.M. Soil Mechanics and Foundation Engineering, **2015**, *52(1)*: 18–22.
18. Tarasenko, O.S., Bodryshev, V.V., Abashev, V.M. *Bulletin of Tula State University. Technical Science*, **2017**, *2*, 290–302.
19. Tarasenko, O.S., Bodryshev, V.V., Abashev, V.M. *Electronic Journal "Transactions of Moscow Aviation Institute",* **2015**, *83,* http://trudymai.ru/published.php?ID=62032, accessed 20 April 2019.
20. Volkov, V.F. *International Conference on the Methods of Aerophysics Research.* Novosibirsk, Russia, **1998**, 228–233.
21. Volkov, V.F., Derunov, E.K. *Physics Engineering Journal*, **2006**, *79(4),* 81–90.
22. Volkov. V.F., Derunov. E.K. *Computational Methods and Programming*, **2005**, *6(1),* 75–85.
23. Zabrodin, A.V., Lutsky, A.E., Brodetsky, M.D., Derunov, E.K. *Thermophysics and Aeromechanics,* **1995***, 2(2),* 97–102.

$$sin\alpha=\frac{1}{M_1};\ sin\beta=\frac{1}{M_2} \quad \text{(Eq. 1)}$$

$$\alpha=arcsin(\frac{1}{M_1});\ \beta=arcsin(\frac{1}{M_2}) \quad \text{(Eq. 2)}$$

$$y_0=tg(\alpha)x_0+c;\ y_0=tg(\beta)x_0+d \quad \text{(Eq. 3)}$$

$$x_0=\frac{c-d}{tg(\alpha)-tg(\beta)} \quad \text{(Eq. 4)}$$

$$c=y_1-tg(\alpha)x_1 \quad \text{(Eq. 5)}$$

$$d=y_2-tg(\beta)x_2 \quad \text{(Eq. 6)}$$

$$y_0=(x_0-x_1)tg(arcsin(\frac{1}{M_1}))+y_1 \quad \text{(Eq. 7)}$$

$$x_0=\frac{y_1-y_2-tg(\arcsin(\frac{1}{M_1}))x_1+tg(\arcsin(\frac{1}{M_2}))x_2}{tg(\arcsin(\frac{1}{M_1}))-tg(\arcsin(\frac{1}{M_2}))}$$ (Eq. 8)

$$H_1=y_1-0,5D_1-y_0;\ H_2=y_0+0,5D_1-y_2$$ (Eq. 9)

$$y_3 = y_0+H_1;\ y_4 = y_0 - H_2$$ (Eq.10)

$$x_3= x_0-\frac{H_1}{tg(\varphi)};\ x_4=x_0-\frac{H_1}{tg(\theta)}$$ (Eq. 11)

$$x\cos(\varphi)+y\sin(\varphi)=d$$ (Eq. 12)

$$d=\frac{1}{N}\sum_{i=1}^{N}(x_i\cos(\varphi)+y_i\sin(\varphi))$$ (Eq. 13)

$$\varphi = 2\text{arctg}\left(\frac{1}{2}\frac{N\sum_{i=1}^{N}x_iy_i-\sum_{i=1}^{N}x_i\sum_{i=1}^{N}y_1}{\left\{N\sum_{i=1}^{N}x_i^2-\left(\sum_{i=1}^{N}x_i\right)^2\right\}-\left\{N\sum_{i=1}^{N}y_i^2-\left(\sum_{i=1}^{N}y_i\right)^2\right\}}\right)$$ (Eq. 14)

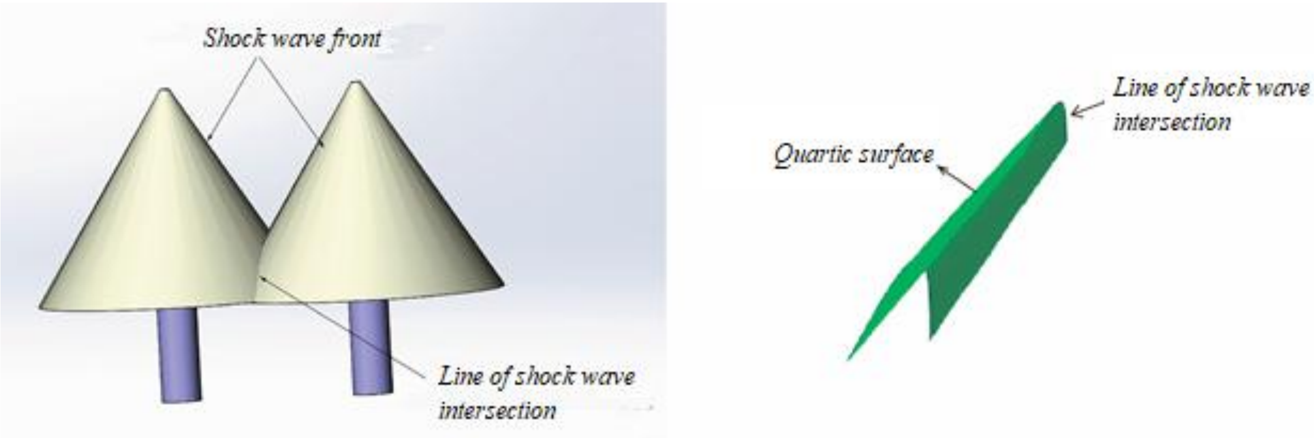

Figure 1. *The geometric pattern of the intersection of shock waves (a) and the surface shape of the compressive shock wave after the intersection of shock waves (b)*

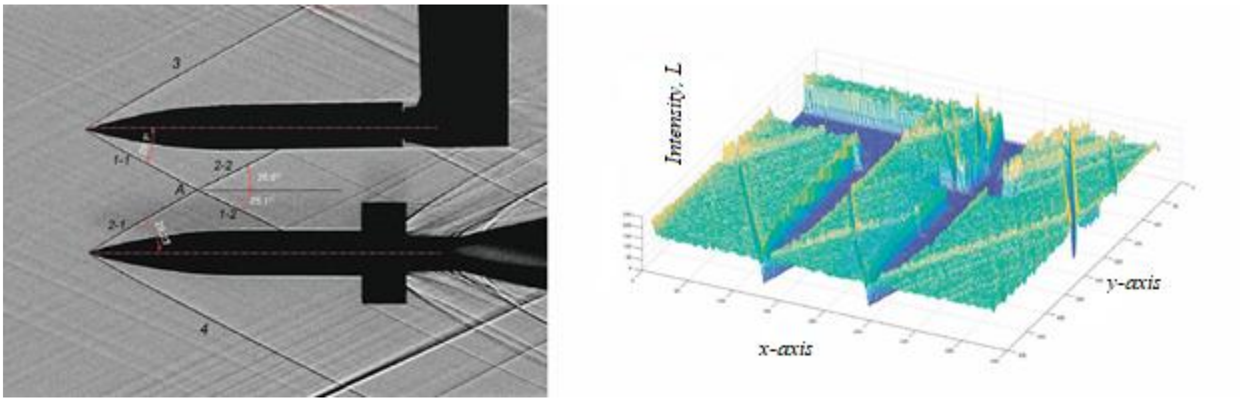

Figure 2. *The video frame of the shock wave intersection zone (a) and the corresponding mapping of the function L=f(x, y) (b)*

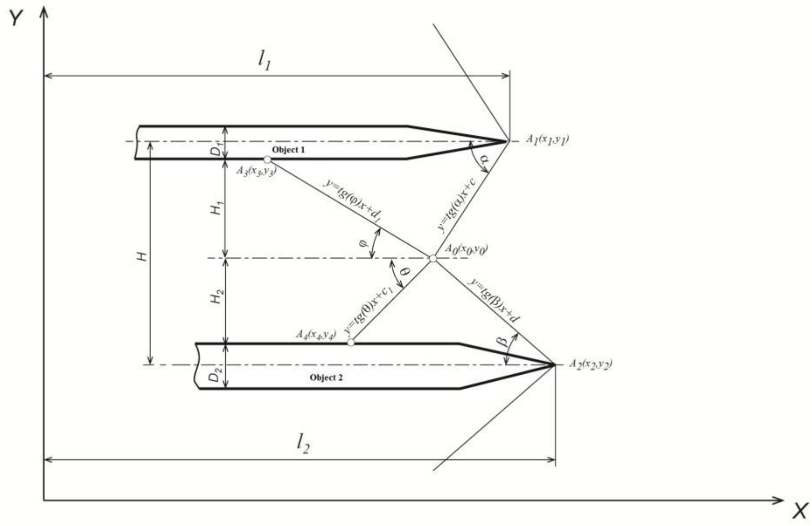

Figure 3. *The pattern of the intersection of oblique conical compressive shock waves*

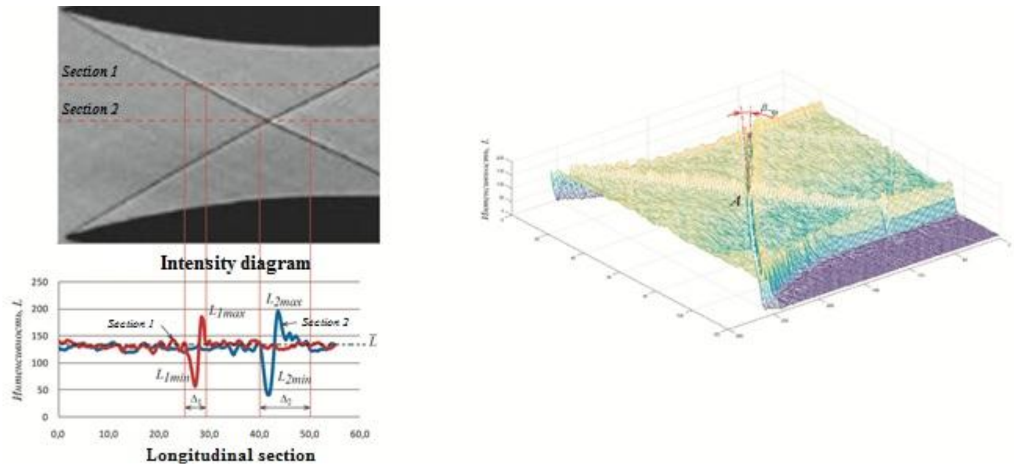

Figure 4. *Dynamics of changes in image intensity in longitudinal sections (a), display of changes in the angle of the shock wave flow after the intersection point (b)*

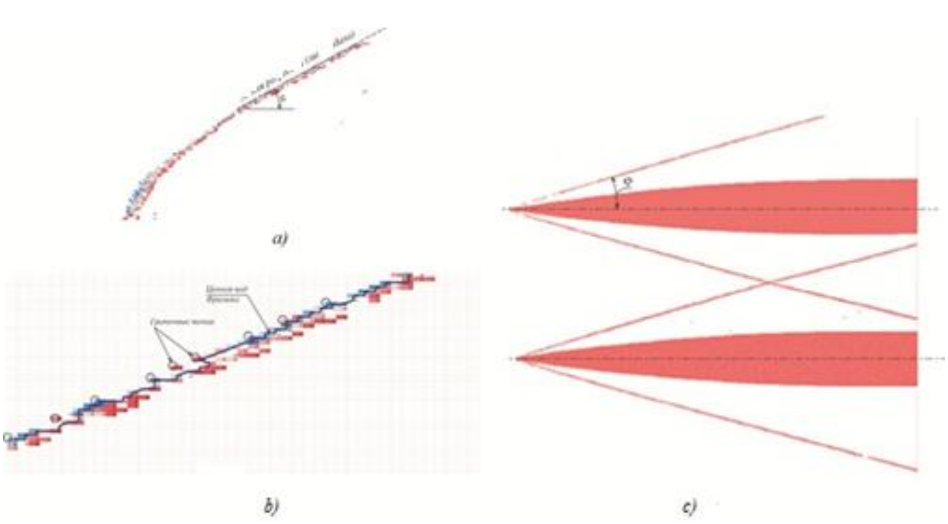

Figure 5. *Example of displaying an array of cells located in the compressive shock wave: a - with the given condition $L_i \geq L_{LV}$, b - on the Mach shock line, c - the pattern of shock waves intersection*